Magnetic second harmonic generation at the Co2MnSi/AlOx interface

doi: 10.1063/1.2841174

Magnetic second harmonic generation at the Co_2MnSi/AlO_x interface

L. R. Shelford,[1,a)] Y. Liu,[1] R. J. Hicken,[1] Y. Sakuraba,[2] M. Oogane,[2] and Y. Ando[2]
[1]*School of Physics, University of Exeter, Stocker Road, Exeter EX4 4QL, United Kingdom*
[2]*Department of Applied Physics, Graduate School of Engineering, Tohoku University, Sendai 980–8579, Japan*

(Presented on 7 November 2007; received 13 September 2007; accepted 17 January 2008; published online 14 April 2008)

We have studied magnetic second harmonic generation (MSHG) at the Co_2MnSi/AlO_x interface. The variation of the MSHG intensity was consistent with the nonvanishing components of the nonlinear susceptibility tensor expected for the (001) cubic surface. The difference in the MSHG asymmetry, the MSHG anisotropy, is found to have maximum value at an annealing temperature of 450 °C, for which similar samples have previously been found to show optimum $L2_1$ site ordering and maximum tunnel magnetoresistance. © *2008 American Institute of Physics*.
[DOI: 10.1063/1.2841174]

Tunnel magnetoresistance (TMR) in magnetic tunnel junctions (MTJs) has received intense interest due to applications in magnetic field sensing and data storage. The TMR value depends largely upon the spin polarization at the interface between the electrode and the tunnel barrier.[1,2] Post-deposition annealing may improve the structural quality of the interface, and the oxidation of the barrier must be carefully optimized. TMR measurements are time consuming, since usually additional lithographic processing is required to form a MTJ, and can be obscured by the presence of pinholes in the tunnel barrier. Measurement techniques capable of characterizing buried interfaces are therefore attractive for rapid screening of buried interfaces. Within the electric dipole approximation, magnetic second harmonic generation (MSHG) is only sensitive to the magnetization at the interfaces of a centrosymmetric crystal.[3] A first study showed a strong dependence of the MSHG in a $Ni_{81}Fe_{19}/AlO_x$ structure upon the oxidation time of the Al overlayer.[4] More recently, the TMR and MSHG intensity were shown to have a qualitatively similar dependence upon temperature and interface composition in MTJ structures with $La_{1-x}Sr_xMnO_3$ electrodes.[5,6]

In this paper, we investigate the effect of annealing temperature and barrier oxidation upon the MSHG from the interface between a Co_2MnSi (CMS) electrode and Al and oxidized AlO_x overlayers. The full Heusler alloy Co_2MnSi is a highly promising material for use in spintronics due to its predicted half-metallic electronic structure[7] and its high Curie temperature [985 K (Ref. 8)]. Indeed, large TMR values of up to 570% have already been observed at low temperature in MTJs with Co_2MnSi electrodes and an amorphous AlO_x barrier.[9,10] For this material, we show that there is a strong correlation between a quantity that we refer to as the MSHG anisotropy and the TMR observed in MTJs prepared under similar conditions.

The MgO(001)/Cr (40 nm)/Co_2MnSi (30 nm)/AlO_x (1.3 nm) samples were grown by inductively coupled plasma assisted magnetron sputtering at room temperature.[10] The CMS films form a cubic structure of (001) orientation with the hard and easy magnetic axes lying parallel to the [100] and [110] crystal axes, respectively.[11] Sample A_x had varied CMS annealing temperature with x=RT (no annealing), 300, 400, 450, and 500 °C, prior to deposition of the Al capping layer. For samples B_{50} and B', the CMS annealing was performed at 450 °C, after which the Al layer was deposited and then plasma oxidized for 50 s. Sample B' also had a second annealing treatment at 250 °C after barrier oxidation. The experimental setup is shown in Fig. 1. A Ti:sapphire regenerative amplifier supplied 100 fs pulses of 800 nm wavelength and energy of 0.5 μJ at an angle of incidence of 45° to the surface. The inset in Fig. 1 shows the relative orientation of the optical polarization and applied magnetic field. The four combinations of the incident and collected optical polarization states probe different components of the nonlinear optical susceptibility tensor that describes the MSHG.[3,12] From here on, we use the notation s, p to refer to incident fundamental polarization, and S, P to refer to collected second harmonic polarization. The collinear 800 and 400 nm components of the reflected beam were spatially separated using Brewster prisms, and the 400 nm light was detected by a digital photon counting system, with background count rate of 20 counts/s.

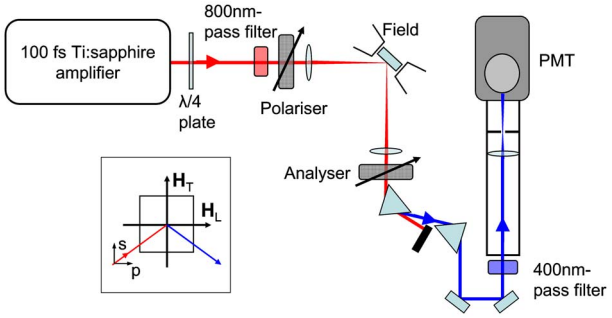

FIG. 1. (Color online) The experimental configuration. The inset shows the relative orientation of the optical polarization and the transverse ($\mathbf{H}_T$) and longitudinal ($\mathbf{H}_L$) magnetic field.

a)Electronic mail: l.r.shelford@exeter.ac.uk.

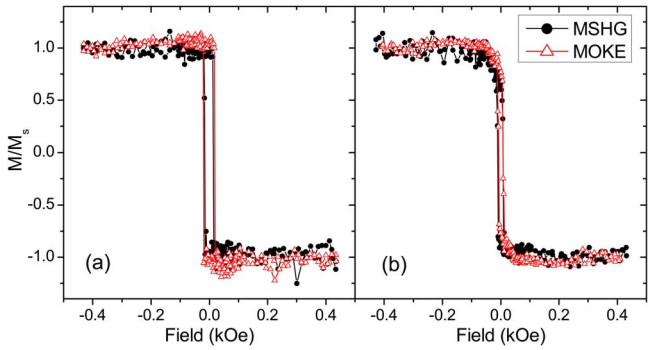

FIG. 2. (Color online) Comparison of linear magneto-optical Kerr effect (MOKE) and magnetic second harmonic generation (MSHG) hysteresis loops for the sample A_{450}, for (a) **H** parallel to [110] and (b) **H** parallel to [100]. Both quantities are normalized to their saturation value.

For cubic crystals, in the electric dipole approximation, SHG is only allowed at the interfaces where the bulk inversion symmetry is broken. For magnetic crystals, time-reversal symmetry is also broken.[12,13] The second harmonic polarization is related to the incident optical electric field and interface magnetization by

$$P_i(2\omega) = \chi^{(2)}_{ijk} E_j(\omega) E_k(\omega),$$

where the nonlinear susceptibility tensor $\chi^{(2)}$ may be written as

$$\chi^{(2)}_{ijk} = \chi^{(2),d}_{ijk} + \chi^{(3),d}_{ijkL} \mathbf{M},$$

where **M** is the magnetization vector. Pan *et al.* give the nonvanishing elements of the cubic (001) surface.[3] The elements have been classified as either odd or even. Odd elements change sign, causing the phase of the second harmonic polarization to change by 180°, upon reversal of the magnetization, while even elements are unchanged. The total signal results from the interference of these odd and even components. The number of tensor elements to be considered may be reduced by the polarization of the incident and collected beams. When the applied magnetic field is swept and the MSHG intensity recorded in a hysteresis loop, the even components determine the average intensity, while the odd components determine the loop height.

In Fig. 2, MSHG and linear magneto-optical Kerr effect (MOKE) hysteresis loops are shown for sample A_{450} for the field applied parallel to the [110] easy and [100] hard axes, in the *p*-P configuration. The MSHG loops were acquired using a field $\mathbf{H}_T$, while the MOKE loops were acquired using a field $\mathbf{H}_L$. The linear MOKE and MSHG loops are seen to have a qualitatively similar shape, suggesting that the bulk and interfacial magnetization reverse in a similar manner.

The effect of annealing temperature and oxidation upon the MSHG response for all samples is shown in Fig. 3. The left and right columns show results obtained with the sample magnetized parallel to the [100] and [110] axes of the CMS, respectively. All measurements were made with the field applied perpendicular to the plane of incidence ($\mathbf{H}_T$ in Fig. 1 inset). The third row [Figs. 3(e) and 3(f)] shows the MSHG asymmetry, $A=[\, I(+\mathbf{M})-I(-\mathbf{M}))/(I(+\mathbf{M})+I(-\mathbf{M})\,]$, which has been suggested to be a more reliable measure of the magnetic contribution to the SHG yield.[12] In the final panel

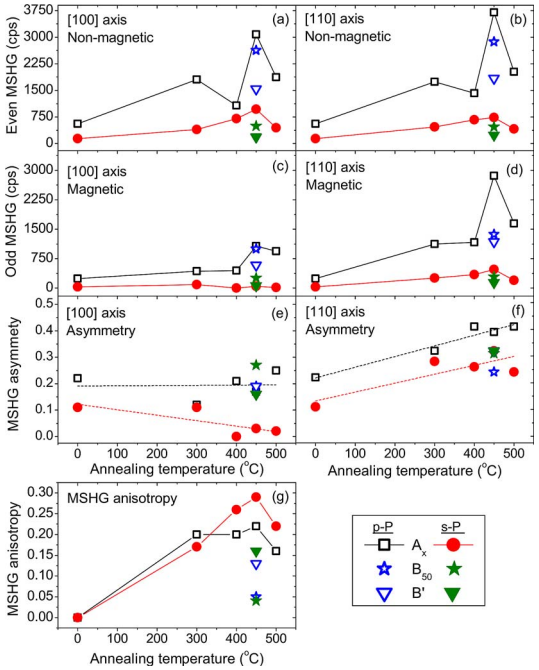

FIG. 3. (Color online) Dependence of MSHG intensity upon annealing temperature. (a) and (b) show the even MSHG yield, (c) and (d) show the odd MSHG yield, (e) and (f) show the MSHG asymmetry, while (g) shows the MSHG anisotropy. The inset in panel (c) gives the symbols used for samples B_{50} and B'.

[Fig. 3(g)], we plot the difference in the MSHG asymmetry for **M** parallel to the [100] and [110] axes, which we refer to as the MSHG anisotropy, defined by $A([110])-A([100])$. Within each panel data are presented for the *s*-*P* and *p*-*P* configurations for all samples (see legend in lower right of figure). No measurable *S*-polarized SHG was observed when the sample was magnetized parallel to either the [100] or [110] axes.

Apart from the *s*-*P* case in Fig. 3(c), all odd and even MSHG intensities exhibit a pronounced peak at an annealing temperature of 450 °C. No such peak is observed in the MSHG asymmetry plotted in Figs. 3(e) and 3(f). Instead, Fig. 3(f) shows a general trend for the MSHG asymmetry to increase with increasing annealing temperature while in Fig. 3(f), the overall trend is for a slight decrease of the MSHG asymmetry with increasing annealing temperature. This implies that the difference in MSHG asymmetry for the easy and hard axes, the MSHG anisotropy, tends to increase for samples annealed at higher temperatures, and indeed shows a peak for an annealing temperature of 450 °C, in Fig. 3(g).

The effect of oxidation (sample B_{50}) and postoxidation annealing (sample B') can also be seen within Fig. 3. From Figs. 3(a)–3(d), the general trend is for both oxidation and the second anneal is to reduce the SHG yield. However, in Figs. 3(e) and 3(f), the effect upon the MSHG asymmetry is much less marked. Finally, in Fig. 3(g), the MSHG anisotropy is seen to first decrease with oxidation and then partially recover after the second annealing.

The full angular dependence of the MSHG asymmetry for samples A_{300}, A_{450}, B_{50}, and B' in the *p*-*P* case is shown in Fig. 4. The samples were gradually rotated through an angle ϕ in the range of 0–360°, about the normal to their

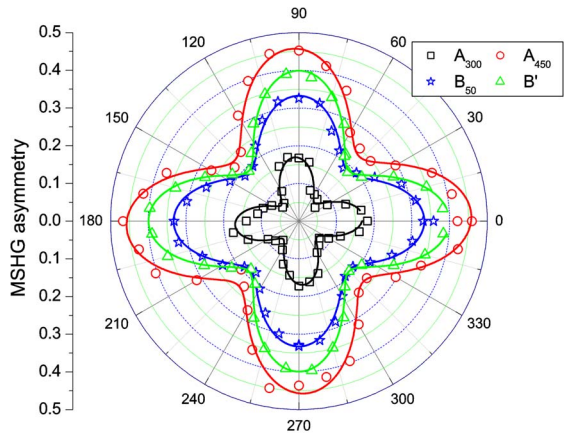

FIG. 4. (Color online) Variation of MSHG asymmetry as the sample is rotated about its surface normal for the *p-P* case. Lines are $\cos(4\phi)$ fits to the data.

plane, for the $\mathbf{H}_T$ field configuration. The experimental data from each sample are well fit by a $\cos(4\phi)$ function, confirming the fourfold symmetry of the interface.

The peak observed in Figs. 3(a)–3(d) and 3(g) occurs at an annealing temperature of 450 °C, which was previously found to yield the optimum degree of $L2_1$ ordering in x-ray diffraction[14] (XRD) and x-ray absorption spectroscopy (XAS) measurements. A multiplet structure observed in the associated x-ray magnetic circular dichroism (XMCD) spectra was suggested to be a signature of the half-metallic state.[15] This annealing temperature also yielded the maximum TMR,[16] suggesting that MSHG may be correlated with surface site ordering and spin polarization at the electrode/barrier interface.

Oxidation of the Al tunnel barrier is known to lead to the appearance of a multiplet structure in the Mn XAS spectra that signifies the formation of Mn oxide,[15] possibly due to migration of oxygen at grain boundaries, which may be responsible for the dramatic decrease of the MSHG anisotropy. Postoxidation annealing leads to a partial recovery of the MSHG anisotropy, which might be expected as oxygen returns from the Co_2MnSi to the tunnel barrier where it is more strongly bound, and perhaps also as the interfacial roughness is reduced. Valev *et al.*[17] observed monolayer-period oscillations in the MSHG yield from a Mn/Co interface, with maximum yield for half-filled monolayers due to an increased interface roughness. They also concluded that the net interfacial magnetic moment is maximum for the flat interface since the MSHG asymmetry is maximum in this case. For the Co_2MnSi/AlO_x interface studied here, the second annealing of sample B' might be expected to reduce the even part of the MSHG intensity as the interface is smoothed, yet, increase the MSHG asymmetry as a result of an increased interfacial magnetic moment. This is indeed observed in Figs. 3(a)–3(g).

We remark that measurements made with different experimental techniques upon the present and equivalent samples may at first sight seem to be at variance. XAS and XMCD studies did not reveal any significant differences between samples B_{50} and B'.[15] In addition, magnetometry and ferromagnetic resonance (FMR) measurements revealed that the magnetization and magnetocrystalline anisotropy decrease, while the damping parameter increases, as the films are annealed at temperatures greater than 300 °C.[11] While further work is required to explain these observations, it is important to remember that MSHG, total electron yield XAS/XMCD, and magnetometry/FMR, probe different regions of the sample, namely, the interface, a near interfacial region of a few nanometer thickness, and the entire volume of the film. MSHG is therefore expected to be most relevant in understanding the variation of measured TMR values, even though *ab initio* calculations of the MSHG are challenging and it is unclear whether any of the experimentally determined quantities can be directly related to either the spin polarization at the Fermi level or to the net interfacial magnetic moment.

The authors would like to acknowledge support from the Engineering and Physical Sciences Research Council (EPSRC).

[1] M. Julliere, Phys. Lett. **54A**, 225 (1975).
[2] J. M. D. Teresa, A. Barthelemy, A. Fert, J. P. Contour, F. Montaigne, and P. Seneor, Science **286**, 507 (1999).
[3] R.-P. Pan, H. D. Wei, and Y. R. Shen, Phys. Rev. B **39**, 1229 (1989).
[4] S. E. Russek, T. M. Crawford, and T. J. Silva, J. Appl. Phys. **85**, 5273 (1999).
[5] H. Yamada, Y. Ogawa, Y. Ishii, H. Sato, M. Kawasaki, H. Akoh, and Y. Tokura, Science **305**, 646 (2004).
[6] Y. Ishii, H. Yamada, H. Sato, H. Akoh, Y. Ogawa, M. Kawasaki, and Y. Tokura, Appl. Phys. Lett. **89**, 042509 (2006).
[7] I. Galanakis, P. H. Dederichs, and N. Papanikolaou, Phys. Rev. B **66**, 174429 (2002).
[8] P. J. Brown, K. U. Neumann, P. J. Webster, and K. R. A. Ziebeck, J. Phys.: Condens. Matter **12**, 1827 (2000).
[9] S. Kämmerer, A. Thomas, A. Hütten, and G. Reiss, Appl. Phys. Lett. **85**, 79 (2004).
[10] Y. Sakuraba, M. Hattori, M. Oogane, Y. Ando, H. Kato, A. Sakuma, T. Miyazaki, and H. Kubota, Appl. Phys. Lett. **88**, 192508 (2006).
[11] R. Yilgin, Y. Sakuraba, M. Oogane, S. Mizukami, Y. Ando, and T. Miyazaki, Jpn. J. Appl. Phys., Part 2 **46**, L205 (2007).
[12] A. Kirilyuk and T. Rasing, J. Opt. Soc. Am. B **22**, 148 (2005).
[13] R. Stolle, K. J. Veenstra, F. Manders, T. Rasing, H. v. d. Berg, and N. Persat, Phys. Rev. B **55**, R4925 (1997).
[14] M. Oogane, Y. Sakuraba, J. Nakata, H. Kubota, Y. Ando, A. Sakuma, and T. Miyazaki, J. Phys. D **39**, 834 (2006).
[15] N. D. Telling, P. S. Keatley, G. v. d. Laan, R. J. Hicken, E. Arenholz, Y. Sakuraba, M. Oogane, Y. Ando, and T. Miyazaki, Phys. Rev. B **74**, 224439 (2006).
[16] T. Daibou, M. Shinano, M. H. M, Y. Sakuraba, M. Oogane, Y. Ando, and T. Miyazaki, IEEE Trans. Magn. **42**, 2655 (2006).
[17] V. K. Valev, A. Kirilyuk, F. D. Longa, J. T. Kohlhepp, B. Koopmans, and T. Rasing, Phys. Rev. B **75**, 012401 (2007).